step and C is approximately expressed by

$$C \sim \frac{2\epsilon_0}{\pi} \ln \csc (\pi d/2b) \text{ farads/meter.}$$

The total energy in the volume element becomes

$$dU_T = \left[\int_A \int \frac{1}{2} \epsilon_0 E^2 dA + CV^2\right] dz,$$

and the power in the z direction is given by

$$\frac{dU_T}{dt} = \left[\int_A \int \frac{1}{2} \epsilon_0 E^2 dA + CV^2\right] \frac{dz}{dt},$$

where dz/dt is the group velocity which is given by $(1/\sqrt{\epsilon_0\mu_0})\lambda/\lambda_g$. Evaluation of the last expression yields (8) of the text.

ACKNOWLEDGMENT

The major part of the work reported in this paper was sponsored by the Bureau of Ships under Contract No. NObsr-39294 and by the Signal Corps under Contract No. DA36-039-sc-42662. It was carried out by the following people of the Polytechnic Research & Development Co., Inc. staff: W. E. Waller, M. Sucher, S. Rubin, L. Kent, C. Kossmann, and the author.

Shielded Coupled-Strip Transmission Line

S. B. COHN†

Summary—**An analysis is made of the odd and even TEM modes on a pair of parallel co-planar strips midway between ground planes. Rigorous formulas are presented for the case of zero-thickness strips, while approximate formulas are given for strips of finite thickness and for strips printed on opposite sides of a thin dielectric sheet supported in air between ground planes (AIL construction). The characteristic impedances and the phase velocities of the two modes are necessary and sufficient information for the design of directional couplers, coupled-line filters, and other components utilizing the coupling between parallel-strip lines. In order to facilitate design work, nomograms are included in the paper which give the dimensions of the coupled-strip cross section in terms of the odd- and even-mode characteristic impedances. The characteristic-impedance scales of these nomograms may be read to an accuracy of better than one per cent over a wide range of values that is sufficient for most purposes.**

INTRODUCTION

NUMEROUS strip-line components utilize the coupling between parallel strips as a basic parameter in their design. Several examples of such components are shown in Fig. 1 (next page), where coupled lines are used to achieve a particular effect in each case. In order to design these circuits to meet prescribed performance specifications, it is necessary to have accurate data on the coupling effects of parallel strips. Solutions for the most important parameters have been obtained, and are presented in this paper.

Fig. 2 (next page) shows transverse field distributions for two fundamental TEM modes that can exist on a pair of parallel conducting strips between parallel ground planes. In Fig. 2(a), strips are at same potential and carry equal currents in the same direction. Because of the even symmetry of the electric field about the vertical axis, this mode will be called the *even* coupled-strip mode. In Fig. 2(b), strips are at equal but opposite potentials and carry equal currents in opposite directions. Due to the odd symmetry of the electric field, this mode will be called the *odd* coupled-strip mode. In the case of the odd mode, the vertical plane of symmetry is at ground potential, and may be replaced by a thin conducting wall joined electrically to the horizontal ground plates. It is clear from the field plots that the capacitance per strip to ground is less for the even case and more for the odd case than for a single isolated strip of the same width. Consequently, the characteristic impedances of the two modes are unequal, being greater for the even than for the odd. In this paper, solutions for the two characteristic impedances will be given.[1] These quantities (plus the mode phase velocities, which are also treated) provide sufficient information for the

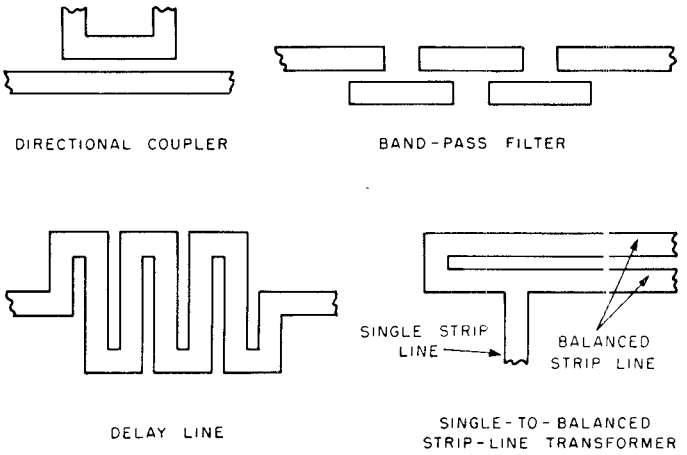

Fig. 1—Several applications of coupled-strip line construction.

† Stanford Res. Inst., Menlo Park, Calif.

[1] (After this paper was prepared, a paper by D. Park appeared with a solution for Z_0 of the odd mode. The use of elliptic-integral identities shows Park's formula to be the same as mine.) D, Park. "Planar transmission lines," TRANS. IRE, vol. MTT-3, pp. 8–12; April, 1955.

design of directional couplers, filters, and other coupled-strip-line components. The graphs and nomograms given in this paper will be of sufficient accuracy for most of such design work.

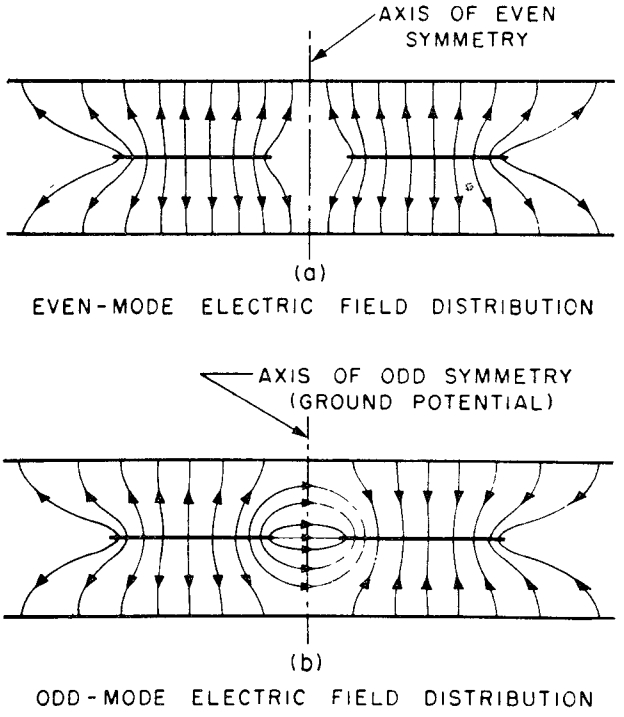

Fig. 2—Field distribution of the even and odd modes in coupled-strip line.

The particular cross sections considered here are shown in Fig. 3. The first, containing zero-thickness strips, is solved rigorously by the conformal-mapping technique. This construction may be closely realized in practice by copper-foil strips sandwiched between dielectric plates that are clad with copper on their outer surfaces. Since the cross section is virtually completely filled with the dielectric material, the phase velocity for both modes is

$$v = c/\sqrt{\epsilon_r}, \tag{1}$$

where c is the velocity of light in free space $(3.00(10)^8$ m/s) and ϵ_r is the relative dielectric constant of the medium in the cross section.

The second cross section in Fig. 3 is of importance in air-dielectric lines, where the thick strips may be supported by spaced dielectric beads, by metallic members at zero-voltage points, or by connectors at the strip ends. The third cross section utilizes foil strips printed on both sides of a thin dielectric sheet supported in air midway between ground plates (AIL construction). Approximate formulas for the second and third cross sections are given in this paper. The phase velocity for Fig. 3(b) is equal to that of light, or, if periodic bead support is used, it is given by (1) where an equivalent ϵ_r is selected to represent the effect of the spaced beads. However, the case of Fig. 3(c) is more complex, since the dielectric constant is not uniform in the cross section. The electric field energy in the dielectric sheet is greater for the odd mode than for the even mode, and therefore the phase velocity for the former will be less than for the latter. An approximate formula is given in this paper for the ratio of these velocities.

Rigorous Formulas for Zero-Thickness Strips

The following exact formulas are derived in Appendix A for the cross section of Fig. 3(a):

$$Z_{0e} = \frac{30\pi}{\sqrt{\epsilon_r}} \cdot \frac{K(k_e')}{K(k_e)} \text{ ohms} \tag{2}$$

where Z_{0e} is the even-mode characteristic impedance measured from *one* strip to *ground*, K is the complete elliptic integral of the first kind, ϵ_r is the relative dielectric constant of the material filling the cross section, and

$$k_e = \tanh\left(\frac{\pi}{2}\cdot\frac{w}{b}\right)\cdot\tanh\left(\frac{\pi}{2}\cdot\frac{w+s}{b}\right) \tag{3}$$

$$k_e' = \sqrt{1 - k_e^2}. \tag{4}$$

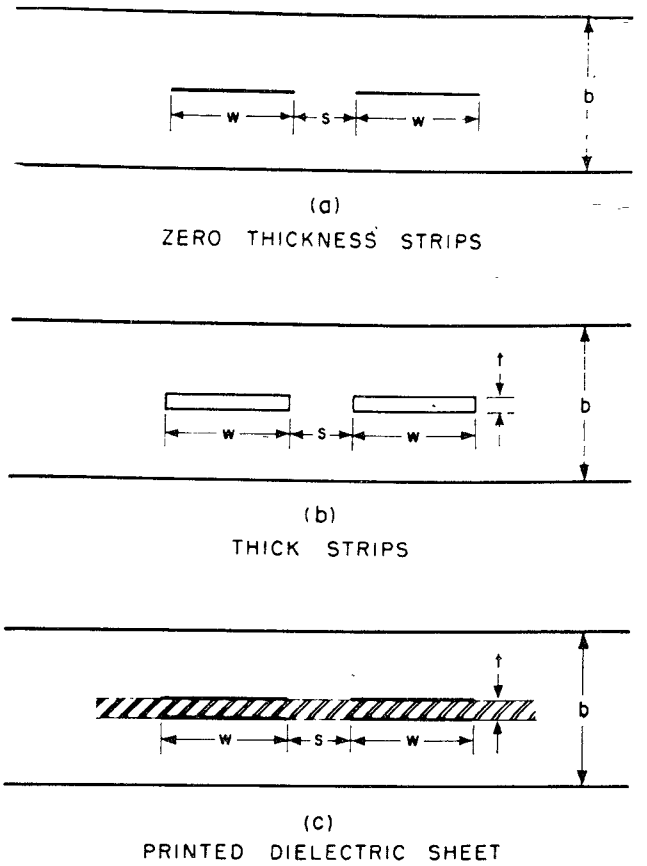

Fig. 3—Coupled-strip-line cross sections considered in this paper.

The variables w, b, and s are dimensions defined in Fig. 3(a). For the odd mode, the characteristic impedance from *one* strip to *ground* is

$$Z_{0o} = \frac{30\pi}{\sqrt{\epsilon_r}} \cdot \frac{K(k_o')}{K(k_o)} \text{ ohms}, \tag{5}$$

where

$$k_o = \tanh\left(\frac{\pi}{2}\cdot\frac{w}{b}\right)\cdot\coth\left(\frac{\pi}{2}\cdot\frac{w+s}{b}\right), \quad (6)$$

$$k_o' = \sqrt{1-k_o^2}, \quad (7)$$

and all symbols are defined as above. If one allows s to become infinite, both Z_{0e} and Z_{0o} reduce to the characteristic impedance of an isolated strip between ground planes. The nature of the dependence of Z_{0e} and Z_{0o} on w/b and s/b is illustrated graphically by Fig. 4.

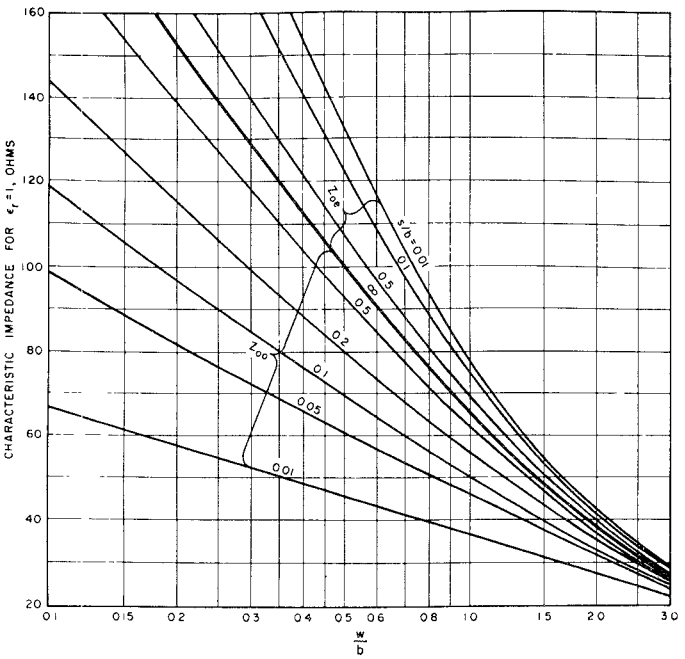

Fig. 4—Graph of Z_{0e} and Z_{0o} vs w/b and s/b.

When a pair of strips are used as a balanced transmission line, the characteristic impedance Z_b measured *between* the strips for the odd-mode distribution is the most useful quantity. This is related to Z_{0o} by

$$Z_b = 2Z_{0o}. \quad (8)$$

In the design of a directional coupler, filter, or other component, Z_{00} and Z_{0e} are first computed to provide the desired circuit performance. Then the dimensions w, s, and b that will yield these characteristic impedances are determined. The following equations are convenient for calculating w/b and s/b,

$$\frac{w}{b} = \frac{2}{\pi}\tanh^{-1}\sqrt{k_e k_o} \quad (9)$$

and

$$\frac{s}{b} = \frac{2}{\pi}\tanh^{-1}\left(\frac{1-k_o}{1-k_e}\cdot\sqrt{\frac{k_e}{k_0}}\right). \quad (10)$$

The parameters k_e and k_o may be obtained as functions of Z_{0e} and Z_{0o} from a single-curve graph of either (2) or (5).

Nomograms for Zero-Thickness Strips

Eqs. (9) and (10) are expressed in nomogram form in Figs. 5 and 6 (pages 32 and 33). In Fig. 5, a straight edge aligned with the specified values of Z_{0e} and Z_{0o} on the outer scales will intersect the proper value of w/b, while in Fig. 6 a similar procedure will yield s/b. These nomograms are designed to be read accurately over a range of Z_{0e} and Z_{0o} large enough for most purposes. In this range, w/b and s/b can be determined with sufficient precision to ensure that Z_{0e} and Z_{0o} will be within one per cent of the desired values.

Fringing Capacitances for Zero Thickness Strips

A quantity of frequent interest is the equivalent fringing capacitance for zero-thickness coupled strips.[2] It will be assumed for simplicity that the strips are wide enough to allow the fringing capacitances at the two edges of each strip to be independent of w/b. This will hold with good accuracy for $w/b \geqq 0.35$, which covers most practical applications. Subject to this assumption, (1) of a previous paper[3] may be written as follows:

$$Z_{0e} = \frac{94.15}{\sqrt{\epsilon_r}\left[\frac{w}{b}+\frac{1}{2\epsilon}\left(C_f'(0)+C_{fe}'\left(0,\frac{s}{b}\right)\right)\right]}\ \text{ohms} \quad (11)$$

and

$$Z_{0o} = \frac{94.15}{\sqrt{\epsilon_r}\left[\frac{w}{b}+\frac{1}{2\epsilon}\left(C_f'(0)+C_{fo}'\left(0,\frac{s}{b}\right)\right)\right]}\ \text{ohms} \quad (12)$$

where $\epsilon = 0.0885\ \epsilon_r$ in mmf per cm, $C_f'(0)$ is the fringing capacitance from one edge to one ground plane in mmf per cm for a single strip of zero thickness (i.e., for $s/b \to \infty$), and $C_{fe}'(0, s/b)$ and $C_{fo}'(0, s/b)$ are the corresponding fringing capacitances in mmf per cm at the adjacent edges of a pair of strips for the even and odd electric-field distributions. (See the sketches in Fig. 7 on page 34). The following rigorous formulas for the fringing capacitances were obtained by letting $w/b \to \infty$ in the analysis for zero-thickness coupled strips:

$$\frac{C_f'(0)}{\epsilon} = \frac{2}{\pi}\ln 2 = 0.4407 \quad (13)$$

$$\frac{C_{fe}'\left(0,\frac{s}{b}\right)}{\epsilon} = \frac{2}{\pi}\ln\left(1+\tanh\frac{\pi s}{2b}\right) = \frac{s}{b}-\frac{2}{\pi}\ln\left(\cosh\frac{\pi s}{2b}\right) \quad (14)$$

[2] (I have been informed in a private communication that C. A. Hachemeister has previously derived general formulas for these capacitances. His results are in a different form than mine, and their equivalence was not checked.)

[3] S. B. Cohn, "Characteristic impedance of the shielded-strip transmission line," TRANS. IRE, vol. MTT-2, pp. 52–57; July, 1954.

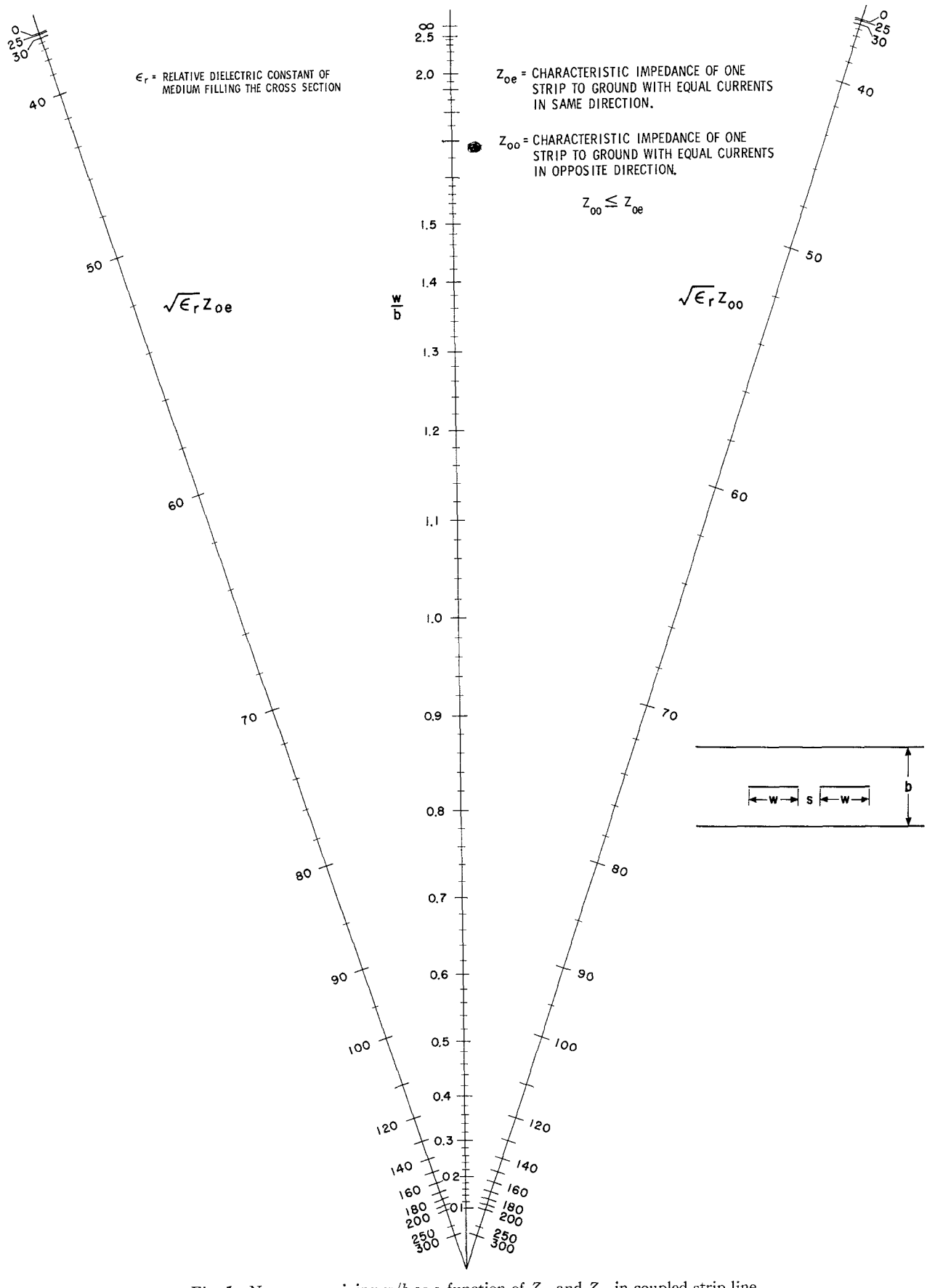

Fig. 5—Nomogram giving w/b as a function of Z_{0e} and Z_{00} in coupled strip line.

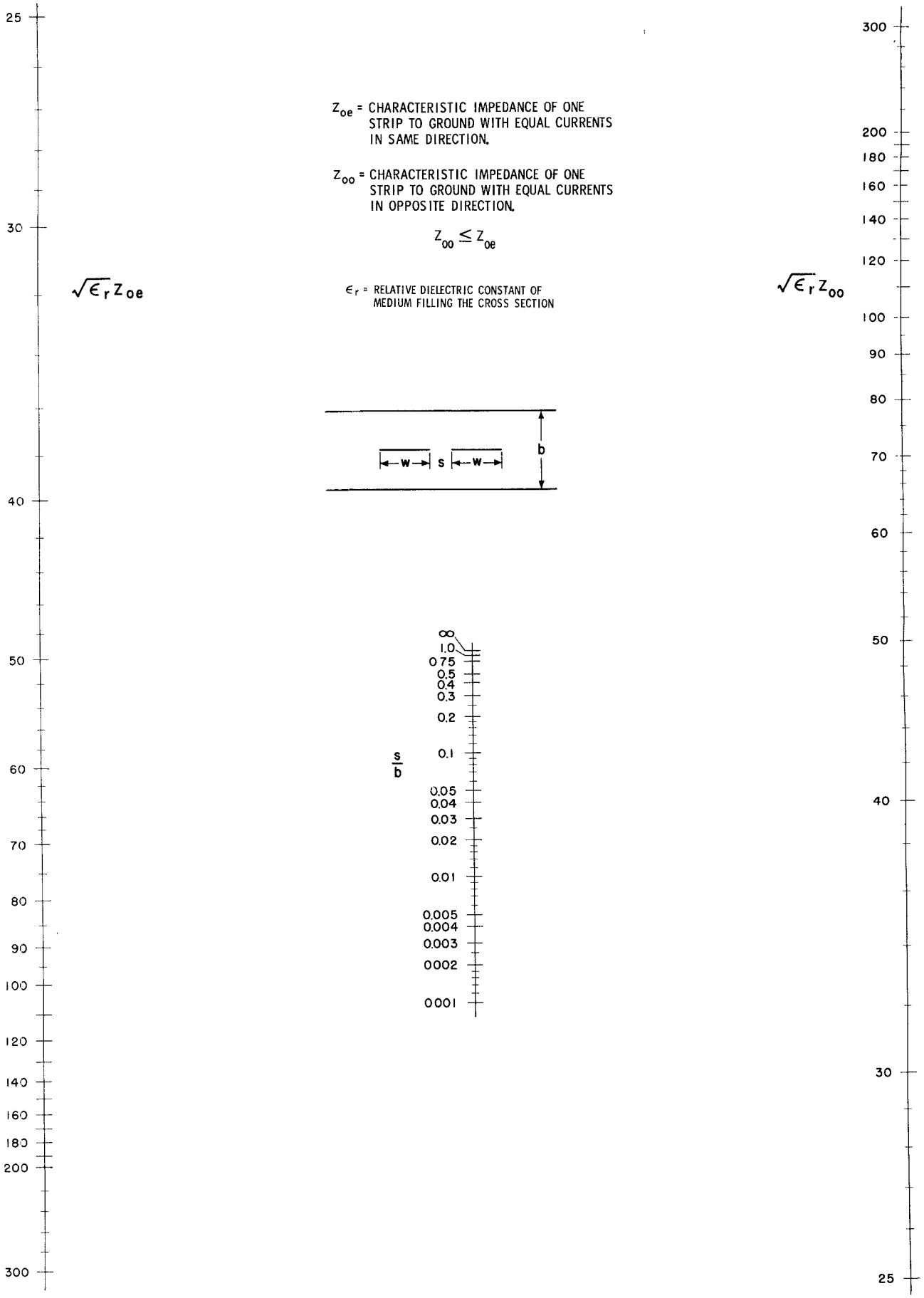

Fig. 6—Nomogram giving w/b as function of Z_{0e} and Z_{00} in coupled strip line.

$$\frac{C_{fo}'\left(0, \frac{s}{b}\right)}{\epsilon} = \frac{2}{\pi} \ln\left(1 + \coth \frac{\pi s}{2b}\right) = \frac{s}{b} - \frac{2}{\pi} \ln\left(\sinh \frac{\pi s}{2b}\right). \quad (15)$$

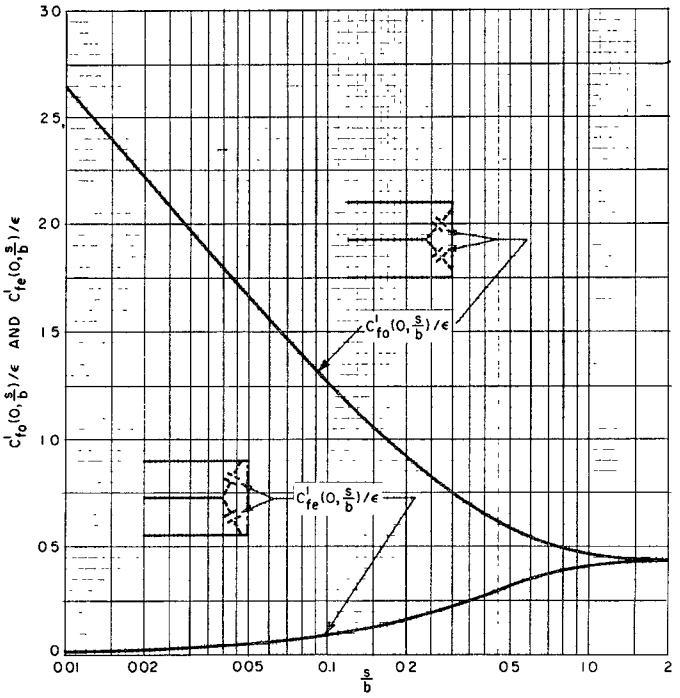

Fig. 7—Fringing capacitances for coupled strips of zero thickness.

Eqs. (14) and (15) are plotted in Fig. 7, where it is seen that they merge into (13) for $s/b \geqq 2$. As $s/b \to 0$, $C_{fe}' \to 0$ and $C_{fo}' \to \infty$. Eqs. (14) and (15) agree, as they should, with Marcuvitz's equivalent circuit for a transverse slit in the common broad wall between two wave-guides.[4] Also, they agree with Oliner's[5] equivalent circuit for a transverse gap in a single strip, which he deduced from Marcuvitz's expressions.

Coupled Thick Strips in Uniform Dielectric

A rigorous solution for coupled thick strips has not been obtained, but the approximate formulas given below should be sufficiently accurate for most purposes. These formulas are based on the solution for zero-thickness strips, and on the fringing-capacitance formula for a thick semi-infinite plate between ground planes. Consequently, the resulting formulas are expected to have their best accuracy for t_b less than about 0.1, and $w/b \geqq 0.35$. However, they may be used with diminished accuracy considerably outside these ranges. In all cases, the phase velocity is given by (1).

[4] N. Maurcuvitz, "Waveguide Handbook," McGraw-Hill Co., Inc., New York, N. Y., pp. 373–375; 1951.

[5] A. A. Oliner, "Equivalent circuits for discontinuities in balanced strip transmission line," Trans. IRE, vol. MTT-3, pp. 134–143; March, 1955.

Even-Mode Case

For the even mode, the characteristic impedance is given by

$$Z_{0e}\left(\frac{w}{b}, \frac{t}{b}, \frac{s}{b}\right) = \frac{94.15 \text{ ohms}}{\sqrt{\epsilon_r}\left\{\frac{w}{b-t} + \frac{1}{2\epsilon}\left(C_f'\left(\frac{t}{b}\right) + C_{fe}'\left(\frac{t}{b}, \frac{s}{b}\right)\right)\right\}}, \quad (16)$$

where $C_f'(t/b)$ is the fringing capacitance for a single thick strip of thickness t.[1] $C_{fe}'(t/b, s/b)$ is the fringing capacitance at the coupled edge of a thick strip in the even mode. The following approximation for $C_{fe}'(t/b, s/b)$ in terms of known quantities is assumed:

$$C_{fe}'\left(\frac{t}{b}, \frac{s}{b}\right) = C_f'\left(\frac{t}{b}\right) \cdot \frac{C_{fe}'\left(0, \frac{s}{b}\right)}{C_f'(0)}. \quad (17)$$

This relation gives the correct result for $t/b \to 0$, $s/b \to 0$, and $s/b \to \infty$. It is expected to give good results throughout the range of interest. Substitution of (17) in (16) (with a certain amount of manipulation) yields the following approximation for Z_{0e}:

$$Z_{0e}\left(\frac{w}{b}, \frac{t}{b}, \frac{s}{b}\right) = \left\{\frac{1}{Z_0\left(\frac{w}{b}, \frac{t}{b}\right)} - \frac{C_f'\left(\frac{t}{b}\right)}{C_f'(0)} \cdot \left[\frac{1}{Z_0\left(\frac{w}{b}, 0\right)} - \frac{1}{Z_{0e}\left(\frac{w}{b}, 0, \frac{s}{b}\right)}\right]\right\}^{-1} \text{ohms}. \quad (18)$$

The values $Z_0(w/b, t/b)$ and $Z_0(w/b, 0)$ are characteristic impedances of single strips, which may be read from a graph in reference [1]. $Z_{0e}(w/b, 0, s/b)$ is the even-mode zero-thickness-strip characteristic impedance given above and $C_f'(t/b)$ and $C_f'(0)$ are fringing capacitances that are also given graphically in reference [2].

Odd-Mode Case

For the odd mode, the following definition for C_{fo}' is assumed when s is large compared to t.

$$C_{fo}'\left(\frac{t}{b}, \frac{s}{b}\right) = C_f'\left(\frac{t}{b}\right) \cdot \frac{C_{fo}'\left(0, \frac{s}{b}\right)}{C_f'(0)}. \quad (19)$$

As in the even mode case, this leads to

$$Z_{0o}\left(\frac{w}{b}, \frac{t}{b}, \frac{s}{b}\right) = \left\{\frac{1}{Z_0\left(\frac{w}{b}, \frac{t}{b}\right)} + \frac{C_f'\left(\frac{t}{b}\right)}{C_f'(0)}\right.$$

$$\left.\left[\frac{1}{Z_{0o}\left(\frac{w}{b},0,\frac{s}{b}\right)}-\frac{1}{Z_0\left(\frac{w}{b},\ 0\right)}\right]\right\}^{-1}\text{ohms.} \tag{20}$$

The definition of terms in (20) is similar to that given for (18).

For s small, (19) can not be expected to be valid, and a better approximation for C_{f0}' is

$$C_{f0}'\left(\frac{t}{b},\frac{s}{b}\right)=C_f'\left(0,\frac{s}{b}\right)+\epsilon\frac{t}{s}, \tag{21}$$

where $\epsilon(t/s)$ is the parallel-plate capacitance across the gap per unit length. Manipulation of (21) gives

$$Z_{00}\left(\frac{w}{b},\frac{t}{b},\frac{s}{b}\right)=\left[\frac{1}{Z_{00}\left(\frac{w}{b},0,\frac{s}{b}\right)}+\left\{\frac{1}{Z_0\left(\frac{w}{b},\frac{t}{b}\right)}-\frac{1}{Z_0\left(\frac{w}{b},\ 0\right)}\right\}-\frac{2}{377}\left\{\frac{C_f'\left(\frac{t}{b}\right)}{\epsilon}-\frac{C_f'(0)}{\epsilon}\right\}+\frac{2t}{377s}\right]^{-1}\text{ohms.} \tag{22}$$

A judicious estimate of the valid ranges for (20) and (22) is $s/t\geqq 5$ for the former and $s/t\leqq 5$ for the latter.

Strips Printed on Dielectric Sheet

For the cross section of Fig. 3(c), (18) should be used for the even-mode case for all s/t, while (20) should yield fair results for the odd mode when $s/t\geqq 10$. However, for $s/t\leqq 10$, the following approximation for C_{f0}' is proposed:

$$C_f'\left(\frac{t}{b},\frac{s}{b}\right)=C_f'\left(0,\frac{s}{b}\right)+\frac{\epsilon_s Z_0\left(\frac{s}{t},\ 0\right)}{377}. \tag{23}$$

The last term in this expression (derived in Appendix B) is the capacitance across the gap due to the field flux inside the dielectric sheet, subject to the assumption that only a tangential component of electric field exists on the dielectric sheet surfaces in the gap region. This assumption gives good results for s/t small, but is poor for s/t large. The quantity $\epsilon_s=\epsilon_0\epsilon_{rs}$ is the absolute dielectric constant of the dielectric sheet, while $Z_0(s/t,\ 0)$ is the characteristic impedance of a shielded single-strip air-dielectric line whose ground plate spacing is t, strip width is s, and strip thickness is zero. $Z_0(s/t,\ 0)$ may therefore be obtained from the characteristic-impedance graph.[1]

Based on (23), the capacitance per strip, and per unit length, for the odd mode is

$$C_{0o}\left(\frac{w}{b},\frac{t}{b},\frac{s}{b}\right)=\frac{377\epsilon_0}{Z_{0o}\left(\frac{w}{b},0,\frac{s}{b}\right)}+377\epsilon_0\left[\frac{1}{Z_0\left(\frac{w}{b},\frac{t}{b}\right)}-\frac{1}{Z_0\left(\frac{w}{b},\ 0\right)}\right]-2\left[C_f'\left(\frac{t}{b}\right)-C_f'(0)\right]+\frac{2\epsilon_0\epsilon_{rs}Z_0\left(\frac{s}{t},\ 0\right)}{377}. \tag{24}$$

The corresponding inductance is not affected by ϵ_{rs}. It can be deduced from C_{0o} by applying elementary transmission-line theory as follows:

$$L_{0o}=\frac{1}{c^2C_{0o}\big|_{\epsilon r=1}} \tag{25}$$

and

$$Z_{0o}=\sqrt{\frac{L_{0o}}{C_{0o}}}=\frac{1}{c}\sqrt{\frac{1}{C_{0o}\big|_{\epsilon rs>1}}\cdot\frac{1}{C_{0o}\big|_{\epsilon rs=1}}}. \tag{26}$$

Therefore

$$Z_{0o}\left(\frac{w}{b},\frac{t}{b},\frac{s}{b}\right)=\left\{\frac{1}{Z_{0o}\left(\frac{w}{b},0,\frac{s}{b}\right)}+\left\{\frac{1}{Z_0\left(\frac{w}{b},\frac{t}{b}\right)}-\frac{1}{Z_0\left(\frac{w}{b},\ 0\right)}\right\}-2\left\{\frac{C_f'\left(\frac{t}{b}\right)-C_f'(0)}{377\epsilon_0}\right\}+\frac{2\epsilon_{rs}Z_0\left(\frac{s}{t},\ 0\right)}{377^2}\right\}^{-1/2}\cdot\left\{\frac{1}{Z_{00}\left(\frac{w}{b},0,\frac{s}{b}\right)}+\left\{\frac{1}{Z_0\left(\frac{w}{b},\frac{t}{b}\right)}-\frac{1}{Z_0\left(\frac{w}{b},\ 0\right)}\right\}-2\left\{\frac{C_f'\left(\frac{t}{b}\right)-C_f'(0)}{377\epsilon_0}\right\}+\frac{2Z_0\left(\frac{s}{t},\ 0\right)}{377^2}\right\}^{-1/2}\text{ohms.} \tag{27}$$

This should give good results for $s/t\leqq 10$.

The phase velocity of the even mode cannot be computed accurately, but will usually be only a per cent or so less than the velocity of light in free space. However, the phase velocity of the odd mode will be affected considerably by the field in the dielectric sheet in the gap region. The following approximate formula gives the ratio of the phase velocities of the two modes.

$$\frac{v_{0o}}{v_{0e}}=\sqrt{\frac{1+2Z_{0o}\left(\frac{w}{b},0,\frac{s}{b}\right)Z_0\left(\frac{s}{t},0\right)/377^2}{1+2\epsilon_{rs}Z_{0o}\left(\frac{w}{b},0,\frac{s}{b}\right)\cdot Z_0\left(\frac{s}{t},\ 0\right)/377^2}}. \tag{28}$$

Appendix A

Derivation of Z_{0e}

Fig. 8 shows the successive transformations used in the conformal-mapping solution for the odd mode in coupled strip line. The solid boundaries denote "electric" (or perfectly conducting) walls, for which $E \times n = 0$ and $H \cdot n = 0$, while the dotted boundaries denote "magnetic" walls, for which $E \cdot n = 0$ and $H \times n = 0$. Therefore, inside the rectangle in Fig. 8(a) the electric and magnetic field lines form a uniform rectangular grid, and in terms of the dimensions of the rectangle shown in the figure, the characteristic impedance of the transmission line whose cross section is the rectangle is given by

$$Z_0 = 120\pi \cdot \frac{K'}{2K} \text{ ohms.} \tag{29}$$

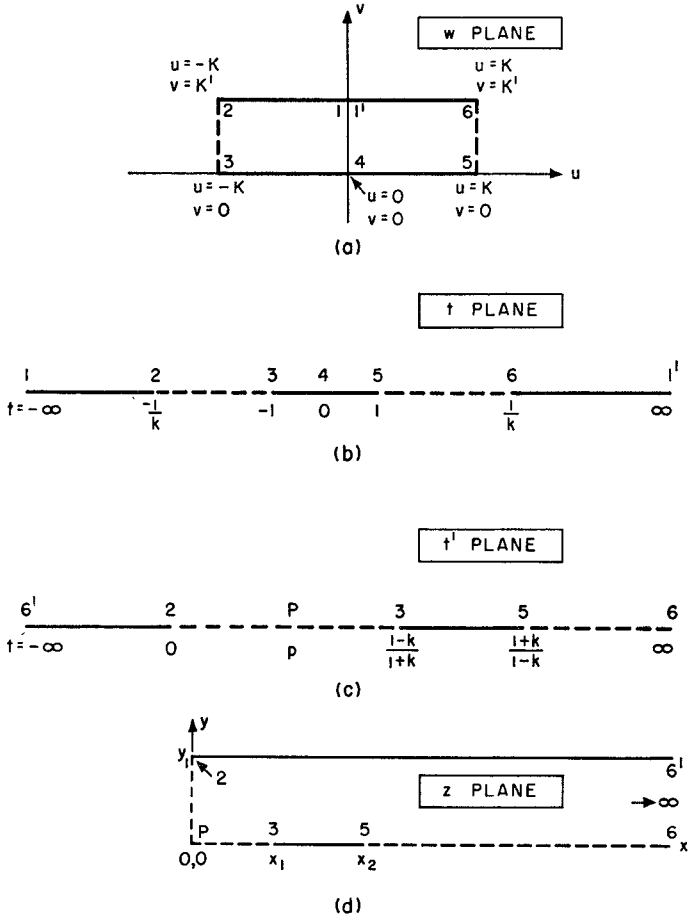

Fig. 8—Transformations used in the derivation of Z_{0e}.

Due to the properties of conformal mapping, the characteristic impedance of a given cross section is not changed by successive analytic transformations. In this derivation, three successive transformations are used: transformation of the region inside the rectangle in the w plane into the entire upper half of the t plane; the upper-half t plane into the upper-half t' plane; and the upper-half t' plane into the bounded region in the z plane shown in Fig. 8(d). Hence the characteristic impedance of the z plane cross section is given by (29). Examination of this cross section shows it to be equivalent to one-quarter of the coupled-strip cross section, and to have the field distribution shown in Fig. 2(a) for the even mode. Thus, Z_{0e} is related to Z_0 by

$$Z_{0e} = \frac{Z_0}{2} = 30\pi \cdot \frac{K'}{K}. \tag{30}$$

It now remains to relate K and K' to the dimensions of the coupled strip line.

The transformation from the interior of the rectangle in the w plane to the upper-half t plane is given by Oberhettinger and Magnus,[6] and the information essential to our purpose is shown in Figs. 8(a) and 8(b). Corresponding points on the boundaries in the w and t plane are indicated by numerals 1 to 6. The coordinates of these points in the two planes are related by

$$K = K(k) \tag{31}$$

$$K' = K(k') \tag{32}$$

where $K(k)$ and $K(k')$ are complete elliptic integrals of the first kind with parameter k and k' respectively. k' is related to k by

$$k' = \sqrt{1 - k^2}. \tag{33}$$

The transformation from the t plane to the t' plane is made purely for convenience, since it greatly simplifies the evaluation of the various constants in the transformation to the z plane. The function used to connect t and t' is

$$t' = \frac{1 + kt}{1 - kt}. \tag{34}$$

This "bilinear" function transforms the upper-half t plane into the upper-half t' plane, and the real t axis into the real t' axis. However, the points on the real t' axis are distributed in a manner better suited for the next step. The coordinates of corresponding points are shown in Figs. 8(b) and (c).

The final transformation to the z plane is carried out by the Schwartz-Christoffel method. This technique is described in various books, such as "Static and Dynamic Electricity," by W. R. Smythe,[7] and therefore the reader will be assumed to be familiar with its principles. The differential equation relating the t' and z planes is

$$\frac{dz}{dt'} = C(t' - t_2')^{\beta_2}(t' - t_6')^{\beta_6}(t' - t_P')^{\beta_P}, \tag{35}$$

where t_n' is the value of t' at the point corresponding to the nth corner in the z-plane boundary, and

[6] F. Oberhettinger and W. Magnus, "Anwendung der Elliptischen Funktionen in Physik und Technik," Springer-Verlag, Berlin, p. 32; 1949.

[7] W. R. Smythe, "Static and Dynamic Electricity," McGraw-Hill Book Co., Inc., New York, N. Y., p. 80 ff.; 1939.

$$\beta_n = \frac{\alpha_n}{\pi} - 1 \tag{36}$$

where α_n is the angle in radians inside the z plane boundary at the nth corner. The values of t_n', z_n, α_n and β_n are summarized below:

Point	t_n'	z_n	α_n	β_n
2	0	jy_1	$\pi/2$	$-\frac{1}{2}$
6	∞	∞	0	-1
P	p	0	$\pi/2$	$-\frac{1}{2}$

thus

$$\frac{dz}{dt'} = \frac{C}{\sqrt{t'-p}\sqrt{t'}(t'-\infty)} = \frac{C'}{\sqrt{t'(t'-p)}} \tag{37}$$

where $C/(t'-\infty)$ is treated as a new constant C'. (This fails only at $t'=\infty$, where it does not matter.) Eq. (37) may be integrated with the aid of a table of inetgrals (e.g., B. O. Peirce[8]):

$$z = C' \cdot 2 \tanh^{-1} \sqrt{\frac{t'-p}{t'}} + C''. \tag{38}$$

We see at once that $C''=0$, since z is required to be zero when $t'=p$. Also, insertion of the corresponding points $z=jy_1$ and $t'=0$ shows that $C'=y_1/\pi$. Hence (38) reduces to

$$z = \frac{2y_1}{\pi} \cdot \tanh^{-1} \sqrt{1-\frac{p}{t'}} \cdot \tag{39}$$

Next, we will substitute corresponding values of t' and z at the edges of the strip.

$$x_1 = \frac{2y_1}{\pi} \tanh^{-1} \left(1 - \frac{1+k}{1-k} \cdot p\right)^{1/2} \tag{40}$$

$$x_2 = \frac{2y_1}{\pi} \tanh^{-1} \left(1 - \frac{1-k}{1+k} \cdot p\right)^{1/2}. \tag{41}$$

But the dimensions b, s, and w of the coupled strip line are related to the z plane dimensions by

$$b = 2y_1, \qquad s = 2x_1, \qquad 2w + s = 2x_2 \tag{42}$$

and therefore

$$\frac{s}{b} = \frac{2}{\pi} \tanh^{-1} \left(1 - \frac{1+k}{1-k} \cdot p\right)^{1/2} \tag{43}$$

$$\frac{2w+s}{b} = \frac{2}{\pi} \tanh^{-1} \left(1 - \frac{1-k}{1+k} \cdot p\right)^{1/2}. \tag{44}$$

It now remains to eliminate p from (43) and (44) and to solve for k. The use of several hyperbolic-function identities leads to the following result:

$$k = \tanh\left(\frac{\pi}{2} \cdot \frac{w}{b}\right) \tanh\left(\frac{\pi}{2} \cdot \frac{w+s}{b}\right). \tag{45}$$

When the subscript "e" is added to k and k' to denote the even mode, (45), (30), (31), (32) and (33) are equivalent to (5), (6) and (7).

Derivation of Z_{0o}

The procedure and transformation functions are exactly the same for Z_{0o} as for Z_{0e}, except that the point P is placed between points 6′ and 2 instead of between 2 and 3 in Figs. 8(c) and (d). Also, point 2 is made to occur at $z=0$, and point P at $z=jy_1$. These changes cause the vertical section of boundary between $z=0$ and $z=jy_1$ to be an electric wall instead of a magnetic wall. As a result, the field inside the z-plane boundary is equivalent to that in the coupled strip line for the odd mode, and

$$Z_{0o} = \frac{Z_0}{2} = 30\pi \frac{K(k')}{K(k)} \cdot$$

After the same steps are carried out as above, the formula for k is found to be

$$k = \tanh\left(\frac{\pi}{2} \cdot \frac{w}{b}\right) \cdot \coth\left(\frac{\pi}{2} \cdot \frac{w+s}{b}\right) \cdot$$

When the subscript "0" is added, (2), (3) and (4) result.

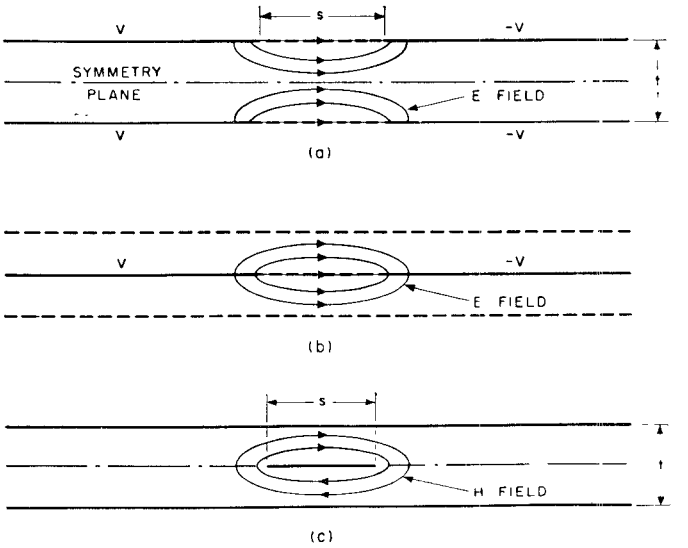

Fig. 9—Equivalence between the region insided a printed dielectric sheet and a shield strip line.

Appendix B

Gap Capacitance in the Printed-Sheet Case

Fig. 9(a) shows the region that is assumed to be equivalent to the printed dielectric sheet in the vicinity of the gap between parallel strip pairs. A magnetic wall may be inserted in the horizontal plane of symmetry without disturbing the field, and then the sepa-

[8] B. O. Pierce, "A Short Table of Integrals," 3rd Edition, Ginn and Co.; p. 18, Eq. 113; 1929.

rated halves of the region can be arranged as in Fig. 9(b) without disturbing the field or the capacitance. Finally, Babinet's transformation is applied to Fig. 9(b), causing all electric and magnetic walls and E and H fields to be interchanged. Thus the E field pattern in (b) is equivalent to the H field pattern in (c). By reversing the direction of the H field lines in the lower half of (c), the magnetic walls on each side of the electric-wall strip may be removed. By Babinet's principle, capacitance per unit length $C_0 = C_{\text{gap}}$ in (b) is related to inductance per unit length L_0 in (c) by $C_0/\epsilon = L_0/\mu$. Then since

$$L_0 = Z_0/c,$$

where c is the velocity of light and Z_0 is the characteristic impedance of the cross section in Fig. 9(c), we may write

$$C_{\text{gap}} = \frac{Z_0}{377^2 c}.$$

However, if the dielectric sheet has a relative dielectric constant ϵ_{rs}, this should be rewritten as

$$C_{\text{gap}} = \frac{\epsilon_{rs} Z_0}{377^2 c} = \frac{\epsilon_0 \epsilon_{rs} Z_0}{377}$$

where Z_0 and c are evaluated for $\epsilon_r = 1$.

High-Power Ferrite Load Isolators

ALVIN CLAVIN†

Summary—**The principles of ferromagnetic resonance have been well described in literature. It is the purpose of this paper to point out the application of these principles to the design of practical microwave components, especially for high power. The various types of ferrite microwave circuits that can be used in the design of a load isolator are presented. The advantages and disadvantages of each of these circuits are discussed in regard to the electrical, mechanical, thermal, and magnetic field requirements. Experimental data are given for the optimum design of nonreciprocal ferrite absorbers for rectangular guide. Finally, practical design information for a power circulator in rectangular waveguide is presented which has been modified for use as a load isolator. This device has extremely high isolations (50 db) and low insertion loss (.5 db), and has maintained an isolation in excess of 30 db over a 25 per cent bandwidth with a permanent magnet field. Power handling ability of 250 kw peak with a .001 duty cycle is easily accomplished without external cooling. This isolator requires quite small magnetic fields for proper operations and hence packaged isolator is quite lightweight. Use of this power circulator for high-power modulators and duplexers is discussed.**

Introduction

THE principles of ferromagnetic resonance at microwave frequencies have been presented by a number of authors.[1–5] It is not the purpose of this paper to elaborate on their work, but instead to discuss the application of the theory to the design of practical microwave components. According to the theory, if an H field is circularly polarized in a plane perpendicular to the magnetization of a ferrite rod or slab, an increasing phase shift and absorption of power occurs as the value of the magnetizing field is made higher. There is a particular value of the magnetizing field which brings the ferrite into gyromagnetic resonance whenever the sense of the circular polarization is positive (the same rotational sense as the coil current producing the magnetizing field). At this point, a large amount of power is absorbed from the rf field by the ferrite; however, little is absorbed from a wave having negative sense of circular polarization. A plot of the phase shift and power absorption is shown in Fig. 1 as a function of the field strength or rf frequency. This is a typical resonant dispersion curve and it should be noted that it is possible to obtain phase shift with very little power absorption

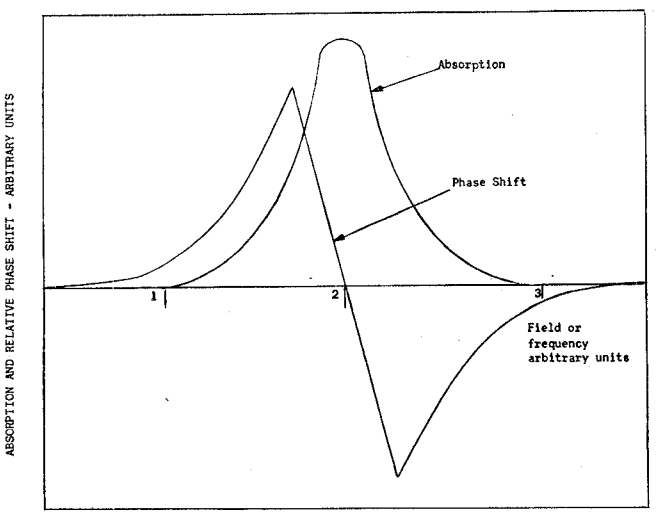

Fig. 1—Relative absorption and phase shift of positively-polarized wave with respect to the negatively-polarized wave.

† Canoga Corp., Van Nuys, Calif.

[1] C. L. Hogan, "The ferromagnetic Faraday effect at microwave frequencies and its applications," The Microwave Gyrator, *Bell Sys. Tech. Jour.*, vol. 31, pp. 1–31; January, 1952.

[2] J. H. Rowen, "Ferrites in microwave applications," *Bell Sys. Tech. Jour.*, vol. 32, pp. 1333–1369; November, 1953.

[3] H. N. Chait, "Non-reciprocal microwave components," Convention Record of the IRE 1954, part 8.

[4] H. Suhl and L. R. Walker, "Topics in guided-wave propagation through gyromagnetic media, Part I—The completely filled cylindrical guide," *Bell Sys. Tech. Jour.*, vol. 33, May, 1954.

[5] H. Suhl and L. R. Walker, "Topics in guided-wave propagation through gyromagnetic media, Part II—Transverse magnetization and non-reciprocal helix," *Bell Sys. Tech. Jour.*, vol. 33, July, 1954.